

# Geotechnical Investigation of Fracture Patterns in a Rock Mass during Excavation by Blasting

Felix Oppong<sup>1</sup>, Isaac Ahenkorah<sup>2</sup>, Dominic Cudjoe Asebiah<sup>3</sup>, Dominic Barimah Osei<sup>4</sup>

<sup>1&4</sup>Department of Geological Engineering, University of Mines and Technology, Tarkwa, Ghana  
Email: stallion10093@gmail.com, dominic.osei@minex360.com

<sup>2</sup>School of Natural and Built Environments, University of South Australia (UniSA), SA 5095, Australia  
Email: ahenkorahisaac290@gmail.com

<sup>3</sup>Department of Materials Science of Semiconductors and Dielectrics, National University of Science and Technology (MISIS), Moscow, 119991, Russia, Email: kdaeh80@gmail.com

**Abstract**— *Overcharging in rocks (wall faces) during blasting and excavation usually causes damage to rock mass in most mining and quarry industries. This creates blast-induced fractures which can relate with pre-existing fracture pattern thereby increasing sliding and rockfall from the crest and body of an excavated wall. The spacing and orientation of pre-existing fractures are predominant at a small-scale mining (galamsey) site at 'Atta ne Atta', a town near Beposo, in the Western Region of Ghana. Geotechnical field studies were carried out to investigate the possibility of any instability within the area to eradicate the occurrence of an unexpected future wall failure (rockfall). The geotechnical mapping conducted was focused on fracture distribution and spacing. Mean spacing ( $S_m$ ) of existing fractures was calculated and corrections were made to obtain calculated spacing ( $S_c$ ). The scanlines of wall face 001 and wall face 002 intersect with their corresponding strike and dip at  $78^\circ$  and  $80^\circ$  respectively creating a slightly favourable fracture pattern and rock wall stability. The fracture pattern created at Wall Face 003 and Wall Face 004 were unfavourable for rock stability with their corresponding scanlines having a strike and dip of  $67^\circ$  and  $73^\circ$  respectively. The instability of these wall faces (003 and 004) is as a result of parallel orientation of the induced fractures to the strike of the pre-existing fractures. Observations made from the stereographic projections and rose diagram indicate a cluster of fracture patterns with a general strike of NNE-SSW. Hence, the fracture patterns in the study area are composed of favourable (stable) rock mass at some walls and unfavourable (unstable) rock mass at other wall faces due to overcharging of blast holes.*

**Keywords** — *small-scale mining ('galamsey'), wall face, fracture pattern, fracture set, rock mass.*

## I. INTRODUCTION

Generally, blasting through boreholes in rocks are associated with two types of forces that influence the surrounding rock; stress wave loading (the shock wave from the explosion) and explosion gas pressure loading [1]. During detonation, the walls of the blast holes are usually exposed to an immediate high pressure that initiates a shock wave that propagates through the rock mass [1]. Gas pressure loading is also generated after the stress wave and travels with a significantly lower speed but for a longer duration. The shock and stress wave cause a complete damage in a form of fragments around the vicinity of the blast and the gas pressure “later” extends these fractures radially [2].

Blasting in bedrock creates blast-induced fractures that strike parallel to pre-existing fractures in the bedrock. The blast-induced fractures can relate with the pre-existing fracture pattern to increase sliding and rock fall from the crest and body of an excavated wall. This can happen in various extents depending on distribution and frequency of pre-existing fractures, rock properties and fracture infilling [3].

Small-scale mining ('galamsey') trenches are prone to rockfall and rockslide after blasting since detailed geotechnical assessment which can be used to define fracture patterns are not considered. This can therefore affect the stability of engineering designs leading to rockfall and other associated geotechnical engineering problems including high construction cost by reinforcement. In order to safeguard the future existence of communities located near quarry and mining industries in Ghana, it is imperative to undertake a detailed geotechnical assessment of the fracture patterns initiated during dynamic blasting. In this study, the rock mass at a 'galamsey' site at 'Atta ne Atta', a community near Beposo, in the Western Region of Ghana was assessed and analyzed in order to provide a profound geotechnical description of fracture distribution, orientation, spacing

(frequency) and the general stability of a rock mass within the study area.

## II. INFORMATION ABOUT THE STUDY AREA

### 2.1 Location and Accessibility

The 'galamsey' site is located at 'Atta ne Atta', a town near Beposo in the Shama District, Western Region, Ghana. The concession is about 1.7 km away from the Beposo Township. Access to the concession is through a feeder road off Takoradi – Cape Coast highway. The nearest community to this site is 'Atta ne Atta' Township, which is about 1 km away from the site. Fig. 1 is a geological map showing the location of the 'Galamsey' site [4].

The site hosts many illegal mining ventures wholly owned by corporate individuals. It was established to produce gold for small-scale mining industries and aggregate to serve the construction industries in the Western and Central Regions of Ghana. The size of this concession is approximately 10 acres and is predominantly composed of granitic outcrops which are used as a suitable aggregate for construction purposes. Aggregates obtained from these areas are used in the region for surface dressing, asphaltic concrete and concrete works, which have been proven to be very suitable and durable in all cases [4].

### 2.2 Topography, Climate and Vegetation

The area generally has a flat land with an isolated hill at Butre and Banso with height ranging between 20 to 40 metres above sea level between Cape Three Point and Princess Town [5].

The District is found within the South-Western Equatorial Climatic Zone of Ghana. The highest mean temperature is 34 °C which is recorded between March and April, while the lowest mean temperature of 20 °C is experienced in August. Relative humidity is very high averaging between 75 % to 85 % in the rainy season and 70 % to 80 % in the dry season. The District is located within the wettest region in Ghana. It experiences a double maxima rainfall of over 1,700 mm [5].

The area falls largely within the High Rain Forest Vegetation Zone, capturing several hectares of rubber plantation. To a large extent, this contributes significantly to reducing the problem of global warming, since the vegetation serve as a sink for CO<sub>2</sub> emissions.

The study area is also closer to Cape Coast, in the central region of Ghana. Cape Coast is dominated by batholith rock and is generally undulating with steep slopes. There are valleys of various streams between the hills, with kakum being the largest stream. The minor streams end in wetlands, the largest of which drains into the Fosu Lagoon at Bakano. In the northern part of the district, however, the landscape is suitable for the cultivation of

various crops. The metropolis has double maxima rainfall. The major rainy seasons occurs between May to July and the Minor rainy season fall within November to January [6]. Cape Coast is a humid area with mean relative humidity varying between 85 % and 99 %. The sea breeze has a moderately effect on the local climate. The hottest months of the year are February and March, just before the main rainy season, while the coolest months are between June and August [7]. The present vegetation of the municipality consists of shrubs of about 1.5 m high, grass and a few scattered trees. The original vegetation of dense shrubs supported by rainfall, has been replaced by secondary vegetation as a result of clearing for farming, charcoal burning, bushfires and other human activities [6].

### 2.3 Geology and hydrogeology

The site is underlain by rocks of the Birimian intrusion related to the late stages of the Eburnean Orogeny (late Pre-Cambium) series south to southeast areas. The area is characterized by foliated, often magmatic, potash rich granitoid in the form of muscovite/biotitic granite and granodiorite, porphyroblastic biotitegenesis, aplites and pegmatities [2].

The Dixcove granitoid complex is intruded along deep-seated faults in three distinct phases which follow one another from basic to acidic: gabbro-diorite-granodiorite. Although the Dixcove granite has been inferred to be younger than the Cape Coast granite, there is the presence of minor intrusions [8]. However, granites like members of the Dixcove suits have been observed within biotite gneiss of the Cape Coast type in many scattered areas throughout Ghana [9]. This suite consists of quartz diorite, tonalite and trondhjemite, granodiorite, adamellite, and to a lesser degree, granite [9&10]. They are typically hornblende-bearing and are commonly associated with gold mineralization where they occur as small plutons within the volcanic belts (Fig. 1).

As such, the top soil consists mainly of dark grey decomposition products of predominantly lateritic quartzite embedded in clayish silt sand followed by a zone of friable, highly weathered gneissic and mica-schist at depths. Overburden was around 5 m. The granite deposit is an outcrop with an average height of about 43 m above sea level. Conventional open pit is employed to mine the granitic deposit with 11 m benches which serve as the progressing excavation face [4].

Groundwater intrusion into the pit occurs often especially during the rainy season when the water table is high. The groundwater in these areas are predominantly controlled by the presence of secondary permeability due to the presence of fractures within the rock masses [4]. Also, the presence of rivers and streams in the area serves as a source of recharge for the groundwater.

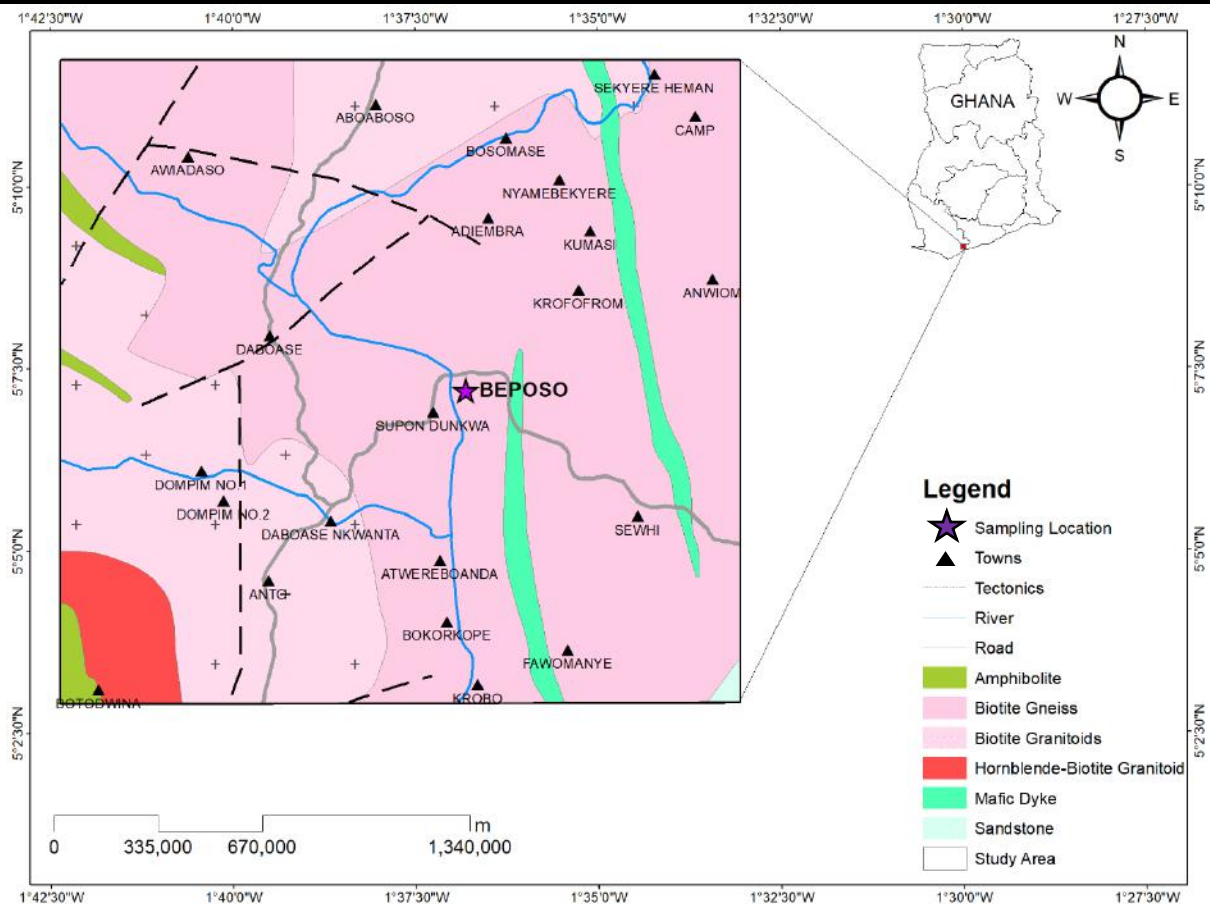


Fig. 1: Geological map of the Southern Part of Ghana showing the Sampling Locations

### III. METHODS USED

Two major methods were used to acquire data and results for this study. These methods include geotechnical field mapping and data collection as well as data analysis.

#### 3.1 Field Mapping and Data Collection

The criteria used for the collection of data in this study was mapping. The mapping exercise was carried out on four separate excavated walls which were selected based on differences in fracture distribution, pattern and spacing. The main emphasis during the mapping exercise was to determine pre-existing or blasting-induced fractures, fracture distribution, fracture spacing (frequency) and fracture orientation present within the selected wall faces. Account of lithology and foliation were also noted, as well as the orientation of any other geological structures, e.g. shear zones. The spacing and orientation of fractures were measured with a hand held Brunton compass and a measuring tape. The Brunton compass was used to measure the strike and dip of the fracture pattern and orientation. The measuring tape was also used to measure the length of spacing between the fractures and the scanline along the face of the walls. The measurement of fracture spacing and orientation was done at four (4) different walls, namely, Wall Face 001, Wall

Face 002, Wall Face 003 and Wall Face 004. Fig. 2 below shows the fracture pattern at the various walls.

#### 3.2 Data Analysis

Fractures that are systematic are classified as a set of fractures. Pre-existing or blast-induced fractures are determined based on the existing surface conditions i.e. how fresh the surfaces are and whether they are open or closed. A closed, narrow and fresh fracture indicates a possible blast-induced fracture. Some of these fractures usually exist close to pre-existing fractures on the excavated wall and are mapped as blast-induced fractures [3].

According to the Rock Mass Rating System [11], discontinuity within rock mass is characterized by a standard stability limit less than 2 m for a non-continuous and unweathered wall rock. Therefore, for a wall face to achieve maximum stability, spacing of fracture set above 2 m will be considered to be favourable in this study. Hence, a defined boundary between the upper (favourable) and lower (unfavourable) limits for standard stability of rock masses has establish in this study as shown in Fig. 3.

The dip and strike of each wall face was illustrated on Stereographic projection and Rose diagram using the

Stereonet 10.0 software [12].

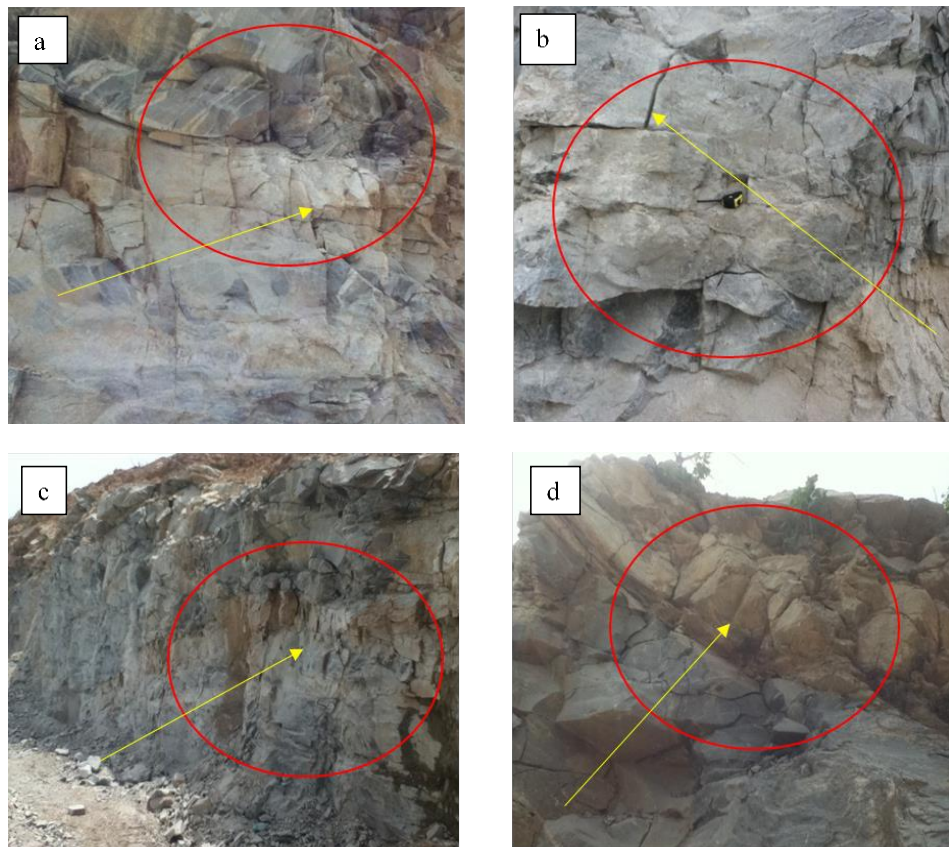


Fig. 2: (a) Fracture pattern at Wall Face 001 (b) Fracture pattern at Wall Face 002 (c) Fracture pattern at Wall Face 003 (d) Fracture pattern at Wall Face 004

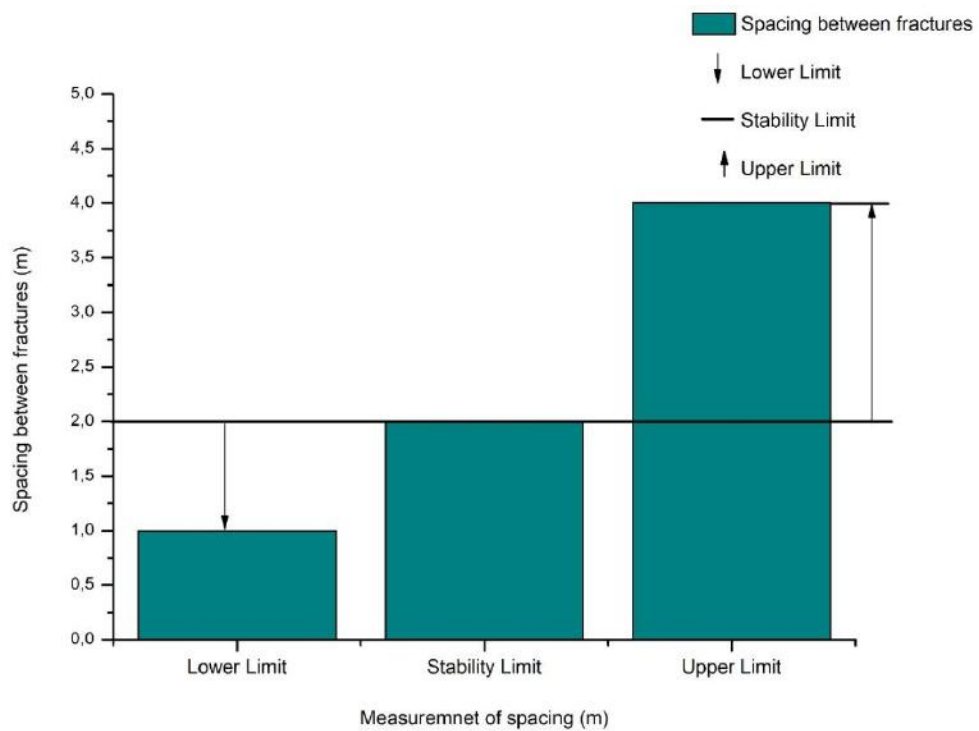


Fig. 3: A Graph of Standard Stability of Fracture Spacing

Mapping of fractures at the various walls gave different orientation of sets. The set of fractures at the various walls has different strikes and dips. Some fracture sets were identified to be parallel to different foliations. The alignment of the fracture sets to the foliations is as a result of the presence of folds yielding a continuous change in strike and dip within the study area.

The spacing (S; given as distance between fractures in m) of fractures were measured in the field by placing a measuring tape of any sort (a scanline), with a given length (L; m) (preferably a few m long depending on fracture frequency) perpendicular to the strike of the fracture set [13].

The measured length along the various walls was 50 m which was at least seven times longer than the spacing. A mean spacing (Sm; m between fractures of the same set) was calculated when the specified measurements are not perpendicular to the strike of the fracture [14]. By counting the number of fractures (N) of a set along the measuring tape, the mean spacing was calculated from the equation:

$$S_m = L/N \tag{1}$$

If spacing measured between two fractures of the same set is not measured perpendicular to the scanline, corrections can be performed to acquire calculated spacing (Sc) by measuring the acute angle ( $\alpha$ ) between the scanline and the strike of the fracture [13]. The mean spacing measured (Sm) in the set is then used to calculate the real spacing from the equation:

$$S_c = S_m \times \sin \alpha \tag{2}$$

In this study the angle for the scanline is the strike of the wall. For the N-S oriented wall the scanline is at different angles [13].

#### IV. RESULTS AND DISCUSSION

##### 4.1 Results

The results of the measurement of fracture spacing and orientation from each excavated wall with their respective mean and calculated spacing as well as the scanline strikes for each wall face are shown in Tables 1 to 4 below.

Table 1: Measurement of Fracture Spacing and Orientation at Wall Face 001

Measurement of Fracture spacing						
Wall Face 001						
The scanline strikes 75°						
Distance from W-E	Strike	Dip	Length	Number of fractures	Mean Spacing	Calculated Spacing
	(°)	(°)	(m)	(N)	(Sm)	(Sc)
1-5	25	21	13.00	5	2.60	1.99
10	35	62	9.00	5	1.81	1.15
15	50	75	7.10	4	1.75	0.73
20	58	60	10.50	6	1.75	0.51
25	31	21	8.00	3	2.66	1.85
30	20	50	2.81	2	1.42	1.14
35	63	42	17.10	5	3.41	0.70
40	52	64	6.22	3	2.00	0.78
45	123	52	9.00	2	4.50	3.34
50	151	14	11.01	6	1.83	1.78

Table 2: Measurement of Fracture Spacing and Orientation at Wall Face 002

Measurement of Fracture spacing						
Wall Face 002						
the scanline strikes 80°						
Distance from W-E	Strike	Dip	Length	Number of fracture	Mean Spacing	Calculated Spacing
	(°)	(°)	(m)	(N)	(Sm)	(Sc)
1-5	48	24	15.40	8	1.92	1.02
10	64	10	24.40	9	2.67	0.73
15	133	5	8.67	11	0.72	0.58
20	155	4	4.60	3	1.53	1.48

25	70	10	11.00	3	3.66	0.64
30	135	67	17.00	7	2.42	1.98
35	22	9	5.60	3	1.86	1.53
40	50	6	9.00	5	1.80	0.90
45	64	13	6.00	5	1.21	0.33
50	72	42	13.01	4	3.25	0.45

Table 3: Measurement of Fracture Spacing and Orientation at Wall Face 003

Measurement of Fracture Spacing						
Wall Face 003						
The scanline strikes 67°						
Distance from W-E	Strike	Dip	Length	Number of Fracture	Mean Spacing	Calculated Spacing
	(°)	(°)	(m)	(N)	(Sm)	(Sc)
1-5	52	35	4.00	3	1.33	0.34
10	22	88	1.80	2	0.90	0.64
15	53	51	11.00	7	1.57	0.38
20	156	74	5.00	11	0.45	0.45
25	50	10	9.00	6	1.50	0.43
30	117	45	15.00	10	1.50	1.14
35	56	87	7.00	4	1.75	0.33
40	76	17	11.00	5	2.20	0.34
45	58	6	3.00	5	0.60	0.09
50	63	15	6.00	4	1.50	0.11

Table 4: Measurement of Fracture Spacing and Orientation at Wall Face 004

Measurement of Fracture Spacing						
Wall Face 004						
The scanline strikes 73°						
Distance from W-E	Strike	Dip	Length	Number of Fractures	Mean Spacing	Calculated Spacing
	(°)	(°)	(m)	(N)	(Sm)	(Sc)
1-5	52	10	3.00	5	0.60	0.22
10	62	35	20.00	6	3.33	0.63
15	68	60	15.00	11	1.36	0.11
20	57	46	5.00	3	1.67	0.45
25	20	37	7.00	5	1.40	1.11
30	126	86	5.00	7	0.71	0.57
35	67	11	8.00	10	0.80	0.08
40	23	6	13.00	8	1.62	1.24
45	73	32	7.00	6	1.16	0.00
50	59	61	11.00	6	1.83	0.44

#### 4.2 Analysis and Discussion of Results

A bar plot showing a graph of mean and calculated spacing of fractures was developed for the various wall faces. The x-axis represents the distance in metres (m) along the wall and the y-axis represents the spacing between fractures in metres (m). A line indicating the

standard stability limit of a wall at 2 m mean spacing between fracture has been presented on each graph. This indicates that, the spacing between fracture at and beyond 2 m is secured for rock stability, however, spacing of fracture below 2 m may result in instability.

From Fig. 4 the scanlines strike  $75^\circ$  with their corresponding strike and dip creating a favourable fracture pattern. The fracture set at a distance of 5 m, 25 m, 35 m, 40 m and 45 m along the wall are above the 2 m spacing of fracture which represents the stability of the wall around these places. The fracture set at a distance of 10 m, 15 m, 20 m 30 m are all below 2 m spacing of fracture were observed to be unstable (below 2 m).

Considering the calculated spacing of the fracture sets, corrections were made for clear estimation of wall stability. The calculated spacing  $S_c$  was used in concluding the results because errors were corrected. As illustrated in Fig. 5, about 90 % of the fracture sets were below 2 m of mean spacing between fractures indicating marginal instability within the Wall face 001. Though only one i.e. the fracture pattern at the distance of 45 m as shown in Fig. 5 exceeded the 2 m spacing of fracture, other sets of fractures were closely below the standard stability limit making it marginally stable. The reason for the marginal stability of these walls by observation is as a result of mineral infillings (quartz veins) in the fractures and which prevents water encroachment between fractures. In addition, by physical observation on the walls, the blast holes were charged with small number of explosives hence small fracture zones were created.

The stereographic projection of the dip and strike of fracture spacing within Wall Face 001 shows a general strike of NNE-SSW (Fig. 6). Observations made from the Rose plot also shows a maximum of 30 % strike between  $051^\circ$  and  $060^\circ$ .

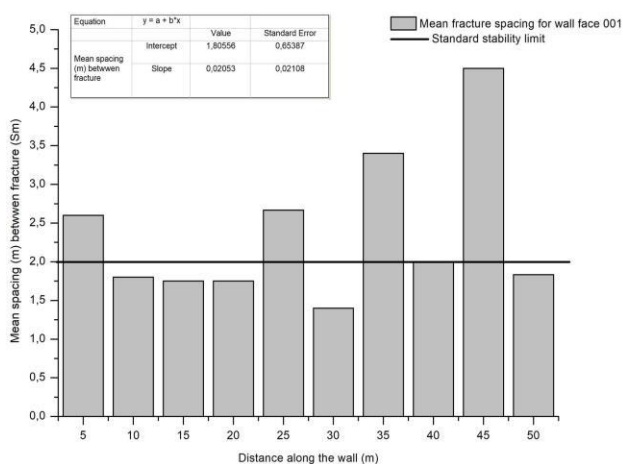


Fig. 4: A Graph of Mean spacing of Fracture at Wall Face 001

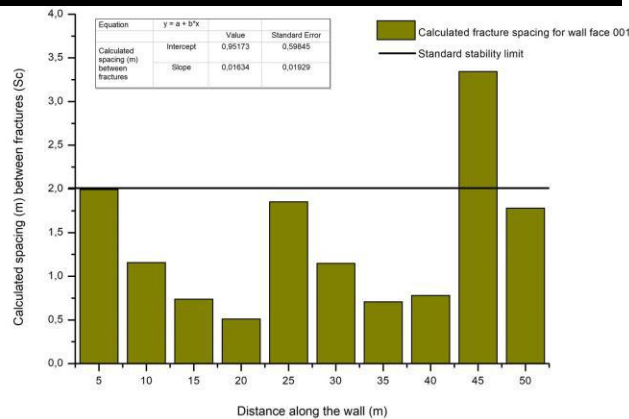


Fig. 5: A Graph of Calculated Spacing of Fracture at Wall Face 001

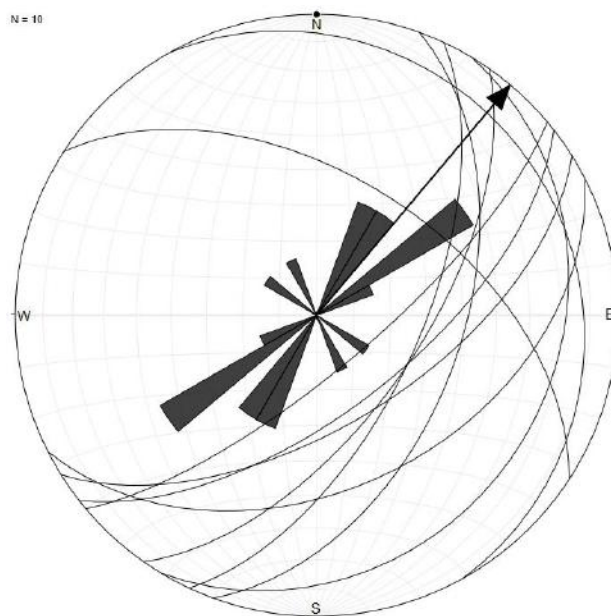


Fig. 6: Stereographic projection and Rose plot for Fracture Spacing at Wall Face 001

From Fig. 7 the scanlines strike  $80^\circ$  with their corresponding strike and dip creating a favourable fracture pattern. The fracture set at a distance of 10 m, 25 m, 30 m and 50 m along the wall are above the 2 m spacing of fracture which represents the stability of the wall around these places, however, other fracture sets were below the 2 m spacing of fracture which indicate unstable condition.

Again, the calculated spacing  $S_c$  was used in concluding the results because errors were corrected. As illustrated in Fig. 8, all the fracture sets were below 2 m of mean spacing between fractures indicating high instability condition within the Wall face 002. Stereographic projection of the dip and strike of fracture spacing within Wall Face 002 also shows a general strike of ENE-WSW. Observations made from the Rose plot also shows a maximum of 20 % strike between  $061^\circ$  and  $070^\circ$  (Fig. 9).

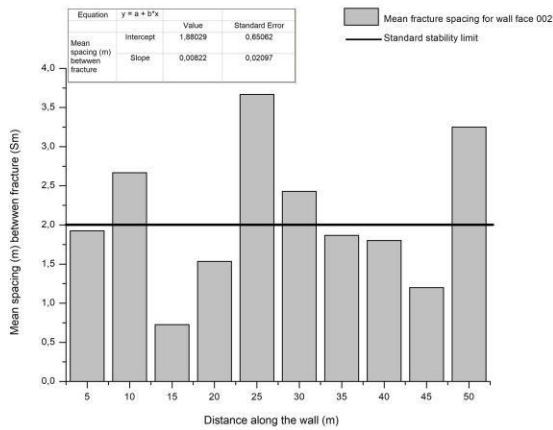


Fig. 7: A Graph of Mean Spacing of Fracture at Wall Face 002

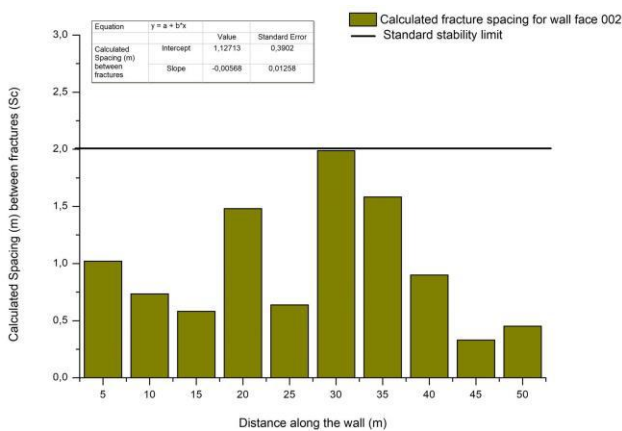


Fig. 8: A Graph of Calculated Spacing of Fracture at Wall Face 002

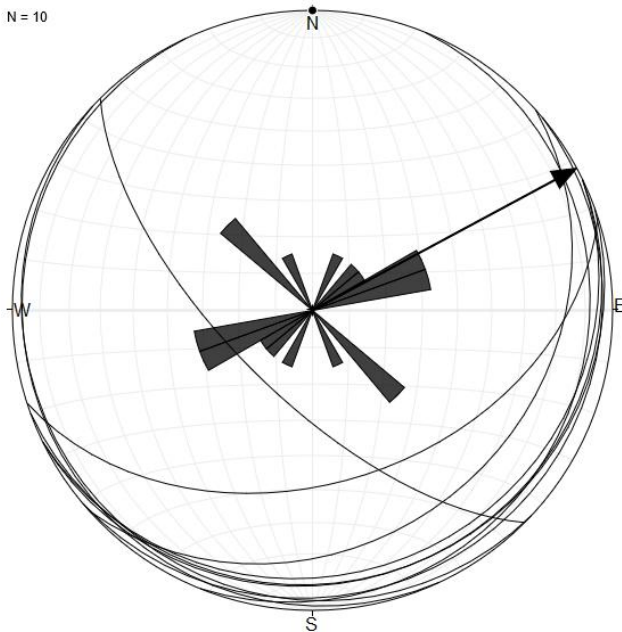


Fig. 9: Stereographic projection and Rose plot for Fracture Spacing at Wall Face 002

As illustrated in Fig. 10 the fracture set along the walls Face (003) at 40 m is are above 2 m spacing of fracture whereas the remaining 9 fracture sets were below the standard stability limit making them walls unstable and vulnerable to failure.

Wall Face 003 recorded the most harmful zones of fracture after estimation using the calculated spacing of fracture sets. Consequently, from Fig 11 all the fractures with their spacing of 0.00-1.24 m and their corresponding strikes created differential unstable parts of the walls which is very unfavourable in response to rock fall and rock slide. Blast induced fractures were observed to be widen as a result of weathering.

Results obtained from the Stereographic projection of the dip and strike of fracture spacing within Wall Face 002 also shows a general strike of NE-SW. Observations made from the Rose plot also shows a maximum of 50 % strike between 051° and 060° (Fig. 12).

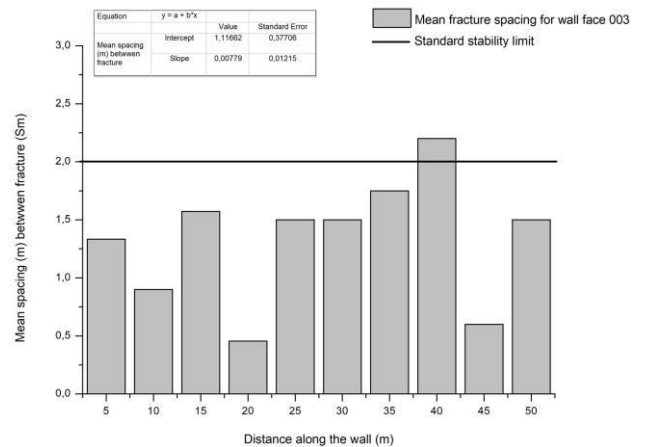


Fig. 10: A Graph of Mean Spacing of Fracture at Wall Face 003

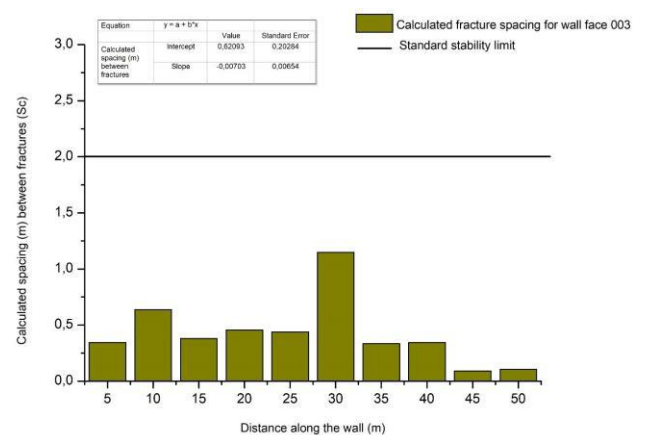


Fig. 11: A Graph of Calculated Spacing of Fracture at Wall Face 003

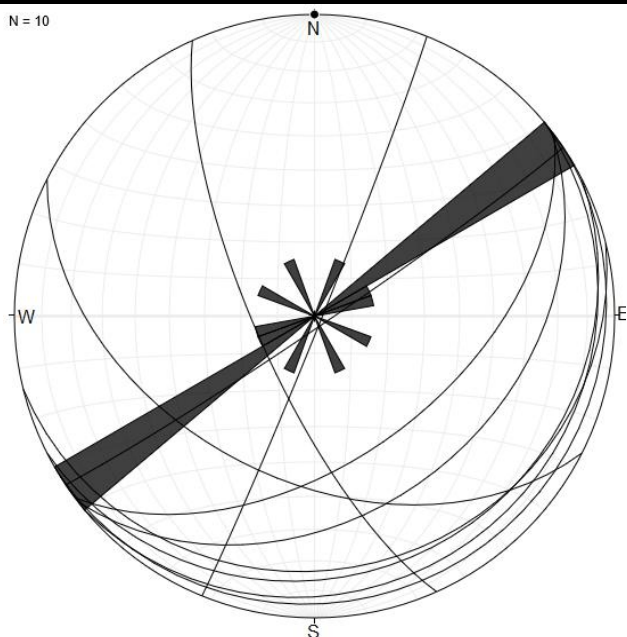


Fig. 12: Stereographic projection and Rose plot for Fracture Spacing at Wall Face 003

Observations made from Fig. 13 show the scanlines strike  $73^\circ$  with their corresponding strike and dip creating an unfavourable fracture pattern. The fracture set at a distance of 10 m along the wall is above the 2 m spacing of fracture which represents the stability of the wall around these places. However, the remaining fracture set were all below 2 m spacing of fracture which indicates high instability within this Wall Face (004).

Again, considering the calculated spacing of the fracture sets, corrections were made for clear estimation of wall stability. The calculated spacing  $S_c$  was used in concluding the results because errors were corrected. As illustrated in Fig. 14, all the fracture sets were below 2 m of mean spacing between fractures indicating high instability within the Wall face 004. The reason for the high stability of these walls by observation is as a result of absence of mineral infillings (quartz veins) in the fractures thereby enhancing weathering of the rock surfaces due to water encroachment between fractures. In addition, by physical observation on the walls, the blast holes were charged with high number of explosives due to the presence of mineralized zones within these areas resulting in the creation of high fracture zones.

The stereographic projection of the dip and strike of fracture spacing within Wall Face 004 shows a general strike of NE-SW (Fig. 15). Observations made from the Rose plot also shows a maximum of 30 % strike between  $051^\circ$  and  $060^\circ$  similar to the strike recorded in Wall Face 001.

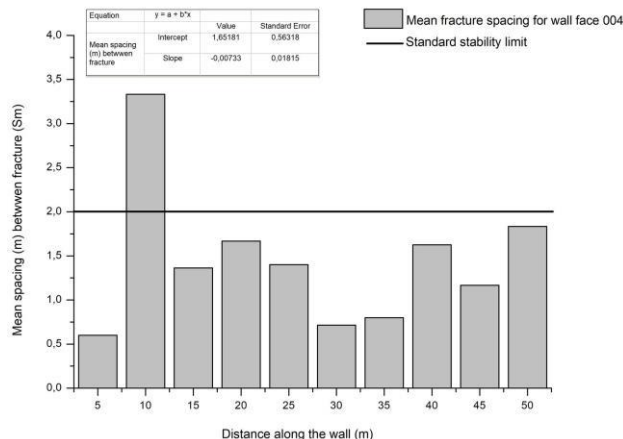


Fig. 13: A Graph of Mean Spacing of Fracture at Wall Face 004

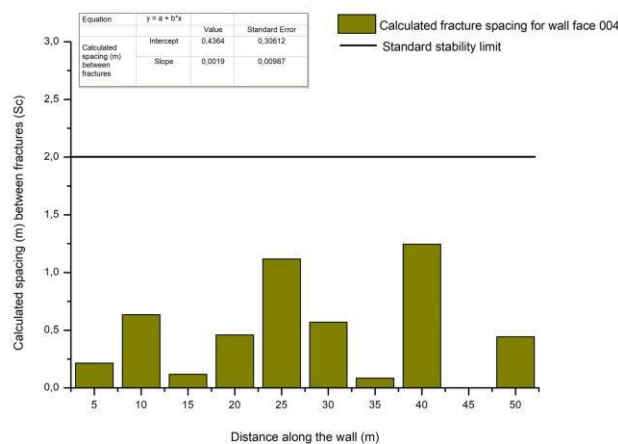


Fig. 14 A Graph of Calculated Spacing of Fracture at Wall Face 004

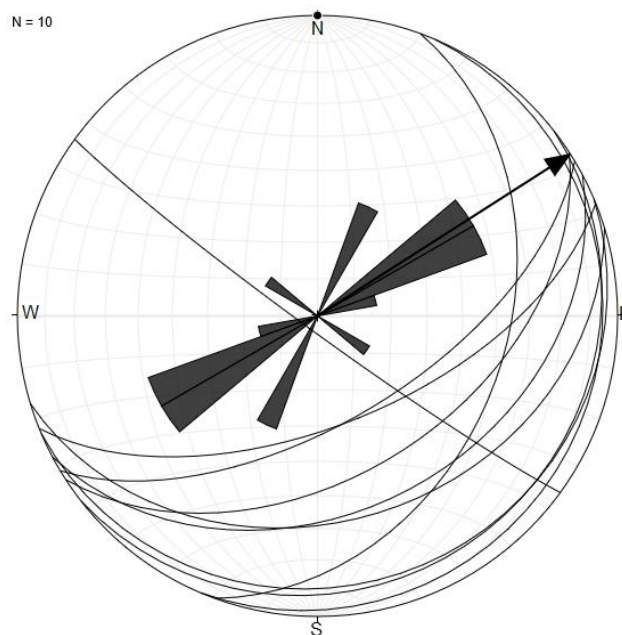


Fig. 15: Stereographic projection and Rose plot for Fracture Spacing at Wall Face 004

## V. CONCLUSIONS AND RECOMMENDATIONS

### 5.1 Conclusions

From the studies and analysis of test results, some conclusions made on the presence of fracture patterns on the outcrops at the site, calculation from the data obtained and general safety of use of the site currently are described below:

- The fracture pattern created at Wall Face 001 and Wall Face 002 are slightly favourable for rock stability. No severe rockfall and rockslide is expected to occur, yet caution is needed when operating around these regions.
- The fracture pattern created at Wall Face 003 and Wall Face 004 are unfavourable for rock stability. The opened blast induced fractures are parallel to the strike of the pre-existing fractures which are exposed to water during rainfall. The infiltration of water usually triggers instability of the wall resulting in rockfall.
- Observations made from the Stereographic projections and Rose diagram indicate a cluster of fracture patterns with a general strike of NNE-SSW with a maximum of 30-50 % strike between 050° and 075°.

### 5.2 Recommendations

It is recommended that:

- Overcharging of blast holes should be avoided.
- The spacing of drill holes at regions of low stability should be wider.
- Drilling at regions of low stability should be done with extreme care.
- Investigation on the walls should be repeated after every episode of blasting.

## REFERENCES

- [1] Rytberg, M., 2015. Significance of Fracture Patterns in a Rock Mass during Excavation by Blasting in Bandhagen, Sweden.
- [2] Zhu, Z., Mohanty, B., Xie, H., 2007. Numerical investigation of blasting-induced crack initiation and propagation in rocks. *International Journal of Rock Mechanics and Mining Sciences* 44, 412-424.
- [3] Mattias Rytberg, (2015), "Significance of Fracture Patterns in a Rock Mass during blasting", Published Degree Project, Department of Earth Sciences, Uppsala University ([www.geo.uu.se](http://www.geo.uu.se)), Uppsala, 2015, pp. 66, 24-22, 11.
- [4] Anon., (2017), "Galamsy Site Operating Plan", Unpublished Annual Report, pp. 3-1
- [5] Ewur, N. E. T., Adupong, R., Eshun, J. D., Mensah, P. A., Nketia, J., & Gormey, B. (2010). Report on Characterization of Coastal Communities and Shoreline Environments in the Western Region of Ghana, Integrated Coastal and Fisheries Governance Initiative for the Western Region of Ghana, USAID Publishers, Ghana, pp. 147-148.
- [6] Faanu, A., Adukpo, O. K., Okoto, R. J. S., Diabor, E., Darko, E. O., Emi-Reynolds, G., Kpordzro, R. (2011). Determination of Radionuclides in Underground Water Sources Within the Environments of University of Cape Coast. *Research Journal of Environmental and Earth Sciences*, University of Cape Coast, Ghana, pp. 270-23.
- [7] Anon. Draft ESIA Report- Onshore Gas Pipeline\_GIP \_100912 | Environmental Impact Assessment | Pipeline Transport. (2012). Retrieved February 9, 2018, from <https://www.scribd.com/document/341552988/Draft-ESIA-Report-Onshore-Gas-Pipeline-GIP-100912>.
- [8] Ahenkorah, I., Awuah, E.M., Ewusi, A., Affam, M., 2018. Geotechnical and Petrographic Characterisation of the Birimian Granitoids in Southern Ghana as an Aggregates for Sustainable Road Construction. *International Journal of Advanced Engineering Research and Science* 5.
- [9] Kesse, G. O. (1985). The Mineral and Rock Resources of Ghana. A. A. Balkema, Publishers, Rotterdam, pp. 610-35.
- [10] Leube, A., Hirdes, W., Mauer, R., & Kesse, G. O. (1990). The early Proterozoic Birimian Supergroup
- [11] Bieniawski, (1989), "Rock Mass Classification-RocScience", [www.rocscience.com](http://www.rocscience.com). Accessed: February 9, 2016.
- [12] Allmendinger, R.W., Siron, C.R., Scott, C.P., 2017. Structural data collection with mobile devices: Accuracy, redundancy, and best practices. *Journal of Structural Geology* 102, 98-112.
- [13] Anon. (1978), ISRM "Suggested methods for the quantitative description of discontinuities in rock masses", *International Journal of Rock Mechanics and Mining Sciences & Geomechanics Abstracts*, Vol. 15, no. 6, pp. 368-319.
- [14] Harrison, J. P. and Hudson, J. A. (2000), "Engineering Rock Mechanics - An Introduction to the Principle", 2nd ed., Elsevier, Oxford, pp. 14-10.